FERMILAB-Conf-03/353 October 2003

FIELD FLATNESS TUNING OF TM_{110} MODE CAVITIES WITH CLOSELY SPACED MODES

L. Bellantoni*, H. Edwards, T. Khabibouline, A. Rowe
Fermi National Accelerator Laboratory**, Batavia, IL, USA

Abstract

Superconducting cavities for the CKM RF separated kaon beamline at Fermilab have modes that are closely spaced compared to the resonance bandwidths when warm, and this complicates the field flatness ("warm") tuning process. Additionally, it is necessary to maintain the azimuthal orientation of the mode during the tuning deformations. We present two analytic techniques to warm-tune cavities with overlapping modes, a finite-element analysis of the tuning process, the design of a warm tuner which maintains mode polarization, and the results of tuning a cavity in which initial manufacturing variations caused the desired π and nearby π-1 modes to be indistinguishable before field flatness tuning.

OVERLAPPING MODES

Because of application [1] requirements, CKM cavities are designed with an aggressive specification for mode spacing. The desired mode is just over 1 MHz from the nearest other mode; at a Q of ~5000 at room temperature, this is just over one bandwidth. Production errors on the first prototype resulted in a cavity for which these two modes were initially indistinguishable, although they could be somewhat resolved by cooling the cavity to liquid N_2 temperatures (see figures 1 and 2).

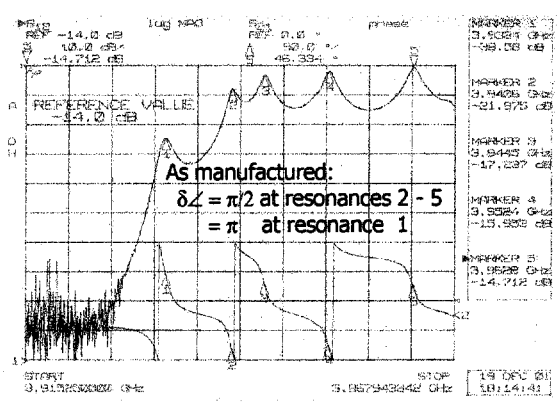

Figure 1. Room temperature S_{21} before tuning.

In order to warm-tune with overlapping modes, one must first realize that the traditional bead-pull formula [2] gives the shift in each of the overlapping resonances. The usual procedure is to measure the phase of S_{12} as the bead moves through the cavity; the phase changes for each of the resonances then add linearly, at least to lowest order. These phase changes may be computed in a reasonably straightforward way from the observed intermode spacing, resonance Q, and S_{21} amplitudes. Two details are noteworthy: (1) the frequency of the resonance is most accurately determined by looking for a peak in $-\partial\phi/\partial\omega$, as in figure 2, and (2) Q is best determined from the left side of peak 2 in figure 1 (theoretical differences in Q between modes are small).

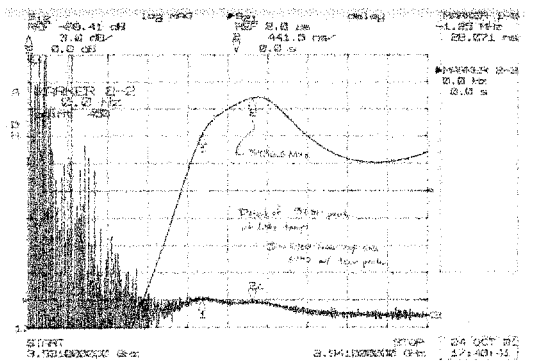

Figure 2. LN_2 temperature S_{21} before tuning.

Alternately, one may calculate S_{21} as a function of frequency directly in the HFSS finite element package, for an empty cavity and then for a cavity with a small metal element at the center of each cell. Again defining the resonance as the peak in $-\partial\phi/\partial\omega$, the frequency shift due to pulling the bead through the cavity may be predicted.

The two methods give broadly similar results. In particular, the shift in S_{21} is the same for a bead in cell *i* as it is for a bead in cell *(N-1)-i*. This is despite the fact that although the π and π-1 modes constructively interfere in the cells 1 through *N/2*, they destructively interfere in cells *N/2* through *N*.

The HFSS result is the one used to define the goal for field-flatness tuning. We have designed an apparatus to pull a bead through a cold cavity to confirm that the effect of the nearby mode has been correctly compensated for.

FINITE ELEMENT ANALYSES

A structural FEA (using the IDEAS package) was performed on a 3-cell half-model of the cavity to predict the mechanical deformation of the cavity cell. These deformations could be easily parametrized analytically and thereby imported into an electromagnetic FEA to

* bellanto@fnal.gov
** Work supported by the U.S. Department of Energy under Contract No. DE-AC02-76CH03000

predict (using the MAFIA package) the resultant RF resonance change during both compression and expansion tuning. Several different schemes for applying pressures to the cavity were evaluated in this way and these evaluations were a primary input in selecting a particular tuning scheme. We sought to have a relatively low change in resonant frequency per millimeter of longitudinal deformation, low change in the inter-cell coupling (equivalently, minimal change in the iris curvature), minimal applied forces and to maintain the polarization of the TM_{110} mode in which the cavities operate.

The optimal compression tuning method is shown in figure 3. Applying pressure to a small annulus near the iris creates a large moment arm between the pressure area and the bending region near the equator arc, providing the mechanical advantage necessary for a low force to deformation ratio.

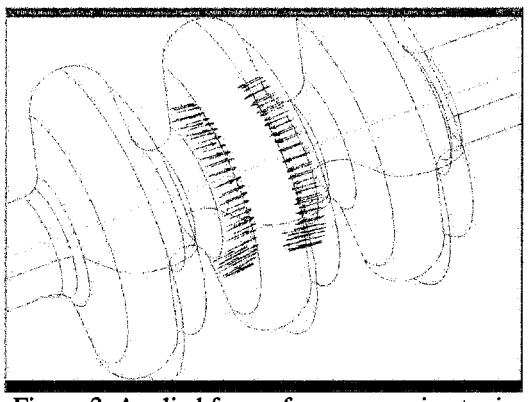

Figure 3: Applied forces for compressive tuning.

The clamping force required to compress a cell with 1.6mm thick walls to the elastic limit of niobium is approximately 840 lbs, resulting in the deformation shown in figure 4. Forces applied in excess of 840 lbs result in the permanent plastic deformation needed to tune the cavity.

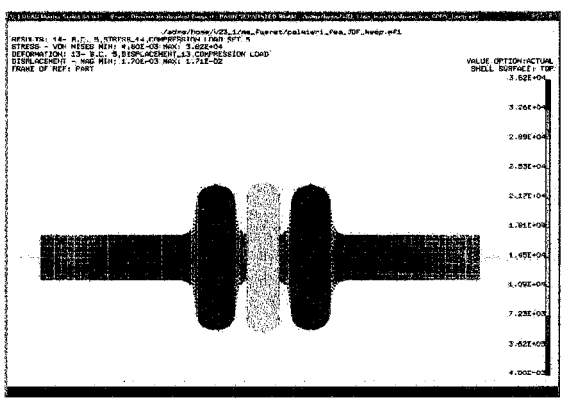

Figure 4: Von Mises stresses and resulting deflection for compressive tuning.

The cell geometry is given by five parameters: the cell length, the diameters of the iris and the equator, and the curvatures of the iris and equator. After analytic parameterization of the deformation shown in figure 4 in terms of these five numbers, the effect of the deformation on the cavity's resonant frequency was found. In the finite element RF package MAFIA, the automesh facility with *r-z* geometry was used. It is important to manually verify that the mesh creation algorithm does not change the number of mesh lines produced over the range of deformations simulated. A single cell was simulated with periodic boundary conditions.

The result of the simulation is that $\partial f_{cell} / \partial Z_{ir} = 47.9$ GHz/m, where the frequency change is per-cell (rather than per-cavity) and Z_{ir} is one-half the length of the cell. We also calculated the change in the cell-to-cell coupling constant, as determined by fitting a sinusoidal dispersion curve to the spacing between the 180° and the 165° phase advance results. Initially 9.25×10^{-3}, this number was reduced by 30.0% per mm.

In expansion, because stiffening rings or other mechanical mounts are not incorporated in the cavity design, tuning occurs as a by-product of pulling on cells adjacent to the cell being tuned. The optimal expansion tuning method limits adjacent cell deformation rather than maximizing the deformation of the tuned cell. It applies a uniform pressure to the tangent surface connecting the iris and equator arcs on adjacent cells. An unfortunate by-product is that the iris is stretched; without stiffening rings, the stretching force must be transmitted through the iris to stretch the tuned cell. Figure 5 shows the resulting stresses and deformations.

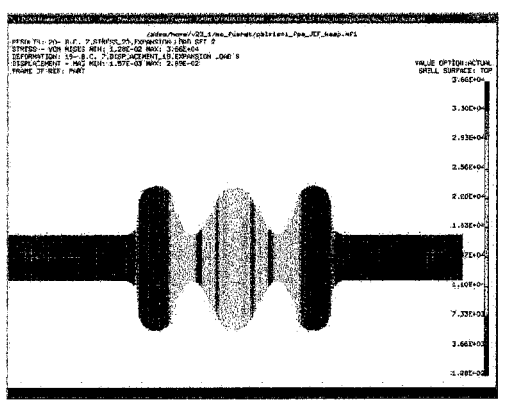

Figure 5. Von Mises stresses and resulting deflection for expansive tuning.

The total pulling force is 960 lbs; $\partial f_{cell} / \partial Z_{ir} = 27.2$ GHz/m, and the cell-to-cell coupling increased by 8.4% per mm.

MECHANICAL TUNING DEVICE

The field-flatness tuning mechanism is shown in figures 6 and 7. It consists of a stable frame holding a set of rails that engage and disengage tuning jaws which contact the

cavities. The contact locations are accurately controlled under the predicted forces. To maintain polarization during the tuning process, four sets of jaws were used. The polarization of the cavity can be changed easily by deforming the iris in a way that is (inadvertently) not azimuthially symmetric. To prevent this, the jaw pairs are closed individually until they contact the cavity and then the four pairs are closed together.

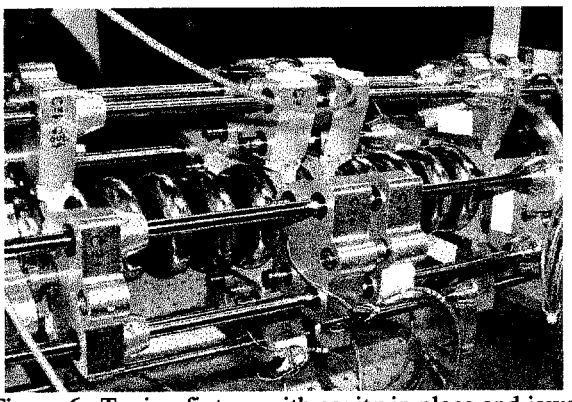

Figure 6. Tuning fixture with cavity in place and jaws engaged.

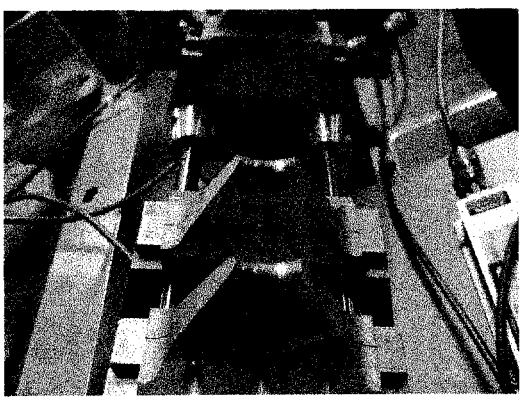

Figure 7. Detail of tuning jaws.

Direct measurement of cell length change was incorporated into the tuning jaws with linear variable differential transformers; a simple hand turned box wrench. applied to a single threaded rod on each jaw set is sufficient to provide the needed tuning pressures. The goal was to provide control of the length of each cell to 0.001"

RESULTS

We were able to warm-tune to a field flatness of about 6%, R.M.S. Our ability to tune more precisely was limited not by the tuning process, but by the mechanical stability of the rather thin-walled cavity structure. Figure 8 shows the target frequency perturbation for each cell as determined by the HFSS simulation of a bead pull, the actual frequency perturbation after tuning, and the frequency perturbation after an initial test at low temperatures. That initial test perforce required some mechanical handling of the cavity. The frequency perturbation at the center of each cell is given by the magnetic deflecting field; there is a node of the electric field at this point. A round 3 mm diameter metal bead was used for this data. We have verified that the result is independent of the bead diameter.

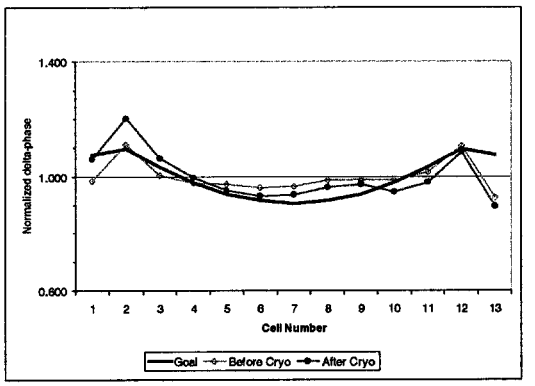

Figure 8. Results of field flatness tuning.

The polarization of the cell is also measured with the bead pull apparatus, but with a dielectric rather than a metal bead. The electric field at the equatorial plane of a cell is, to within a few percent, the same as that for a pillbox cavity. The azimuthial orientation of the field in the cell may then be determined with the simple analytical form $E_z \propto cos(\phi)\, J_1(\rho/\rho_0)$. The data from three bead pulls is needed; one down the center of the cavity, and two displaced 10mm off axis in the $+x$ and $+y$ directions respectively. It is difficult however to determine the polarization of the endcells with this method, because end effects change the fields considerably. Figure 9 shows the bead pull results; analysis of this data shows that we were able to maintain the polarization to 4% R.M.S. This corresponds to about ¼% loss of deflecting power .

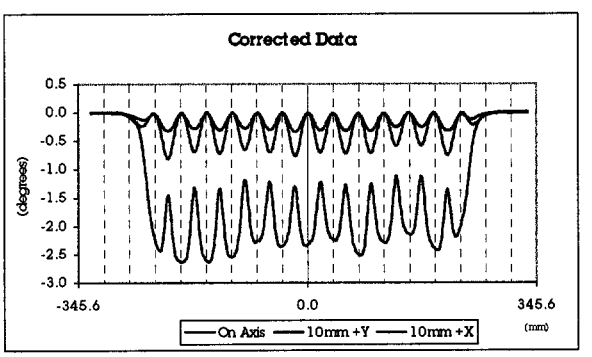

Figure 9. Polarization after field flatness tuning.

Figure 10 shows the S_{21} spectrum after tuning. The data have been shifted to compensate for an overall offset

of 20.897 MHz. This is because the first prototype had to be made without any correction to the forming dies to allow for the effect of springback in the niobium upon the manufactured frequency.

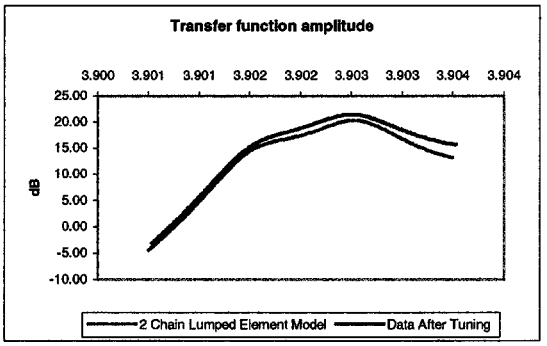

Figure 10. S_{21} after warm tuning, with prediction of two-chain lumped finite element model.

Figure 10 also shows the prediction of a lumped finite element model. This model, described in detail in reference [3], is an elaboration of the work of [4]. In the TM_{110} mode, intercell coupling is provided by the magnetic dipole field in the iris. That field, and the corresponding electric field, are very similar to the field of the TE_{111} mode. An accurate model of the dispersion curve requires that one use two LC resonators for each cell in the cavity to model the two (orthogonal) oscillating modes. In figure 10, this model has been extended to include a resistive term. The two resonators corresponding to the cell nearest port 1 are driven with amplitudes α (for the TM mode oscillator) and β (for the TE mode oscillator) at various frequencies. The plotted quantity is the magnitude of $\alpha A_M + \beta A_E$, where A_M and A_E are the magnitudes of the two oscillators in the cell nearest port 2. The numbers α and β are intended to model the different couplings of the test probes to the two modes. Although they are not precisely known, setting both to 1, as was done in figure 10, reasonably reflects the geometry of the test probes, which were place in the beam pipes, where the fields are basically in an evanescent TE_{11} configuration.

REFERENCES

[1] http://www.fnal.gov/projects/ckm/Welcome.html

[2] e.g., Rimmer and Tigner, "Cavity Measurements" in Chou and Tigner, "Handbook of Accelerator Physics and Engineering", World Scientific, Singapore, 1999.

[3] M. McAshan and R. Wanzenberg, "RF Design of a Transverse Mode Cavity for Kaon Separation", FNAL TM-2144, 22 Mar 2001. Available at [1].

[4] K.L.F. Bane and R.L. Gluckstern, "The Transverse Wakefield of a Detuned X-Band Accelerator Structure", SLAC PUB-5783, March 1992.